

Strained $\text{Si}_{1-y}\text{C}_y$ Thin Films on Si grown by Chemical Vapor Deposition

– new approaches toward high speed MOS devices –

Akira YAMADA, Katsuya ABE, Tatsuro WATAHIKI,
Syuhei YAGI and Makoto KONAGAI

*Department of Physical Electronics, Tokyo Institute of Technology,
2-12-1 Ookayama, Meguro-ku, Tokyo 152-8552, Japan*

Epitaxial $\text{Si}_{1-y}\text{C}_y$ films were grown on Si(001) by chemical vapor deposition (CVD) at substrate temperatures of around 200°C. SiH_4 diluted with H_2 was used as a reactant gas and C_2H_2 , CH_4 or $\text{SiH}_2(\text{CH}_3)_2$ were adopted as a C source gas. The vibration mode at 607 cm^{-1} , which indicated the presence of the C atoms located at the Si substitutional sites, was observed in both Fourier transform infrared absorption and Raman scattering spectroscopy of the samples annealed at 600 to 700°C. The C composition was controlled by varying the C-source gas/ SiH_4 ratio. The maximum substitutional C compositions of 3.5 at. % was successfully obtained.

The ensemble Monte Carlo simulation predicted that the low-field electron mobility of tensile-strained $\text{Si}_{0.99}\text{C}_{0.01}$ is 1.3 times higher than that of Si. Furthermore, the strain effect on the electron transport is more obvious in the velocity-overshoot phenomenon.

1 Introduction

Recently, the group IV alloys such as $\text{Si}_{1-x-y}\text{Ge}_x\text{C}_y$ and $\text{Si}_{1-y}\text{C}_y$ have attracted attention because they are potential new materials which open bandgap engineering in Si technology. Furthermore, the challenge of improving device performance is carried out by enhancement of carrier transport in MOS channel by using $\text{Si}_{1-x}\text{Ge}_x$ /strained Si structure [1]. In this paper, we focus on the Si/strained $\text{Si}_{1-y}\text{C}_y$ structure since $\text{Si}_{1-y}\text{C}_y$ has several advantages compared to $\text{Si}_{1-x}\text{Ge}_x$: We can select many kinds of hydrocarbon gas as a C source for epitaxy of $\text{Si}_{1-y}\text{C}_y$ and they are not toxic, while GeH_4 which is usually used as a Ge source in GS-MBE (gas-source molecular beam epitaxy) is toxic gas. Furthermore, the thermal conductivity of $\text{Si}_{1-x}\text{Ge}_x$ is inferior to that of Si [2].

However, the growth of C-containing epitaxial alloy is difficult due to the very low solid solubility of C in Si. Previous methods for depositing epitaxial $\text{Si}_{1-x-y}\text{Ge}_x\text{C}_y$ and $\text{Si}_{1-y}\text{C}_y$, such as MBE and ultrahigh-vacuum chemical vapor deposition (UHV-CVD), realized Si alloys with only 1–2 at. % C [3, 4, 5, 6]. To date, we have studied the epitaxial growth of Si by mercury sensitized photo-CVD [7], plasma-CVD [8] and HW-CVD [9] at substrate temperatures lower than 200°C. Since the epitaxial growth of Si by these methods proceeds under non-thermal equilibrium conditions, heavy doping can be realized without the solid solubility limitation [10, 11]. In this study, we applied these methods to the growth of $\text{Si}_{1-y}\text{C}_y$ alloy. We firstly describe the electron mobility enhancements in tensile-strained $\text{Si}_{1-y}\text{C}_y$ by using Monte Carlo simulation then demonstrate the epitaxial growth of $\text{Si}_{1-y}\text{C}_y$ by photo- and plasma-CVD.

2 Calculation of electron mobility in strained $\text{Si}_{1-y}\text{C}_y$ by Monte Carlo simulation

Figure 1 shows schematic illustrations of the crystal lattice for strained $\text{Si}_{1-y}\text{C}_y$ on Si, and the subsequent energy splitting of the $\text{Si}_{1-y}\text{C}_y$ conduction band edge. Because the equilibrium lattice constant of $\text{Si}_{1-y}\text{C}_y$ is smaller than that of Si, a pseudomorphic layer of $\text{Si}_{1-y}\text{C}_y$ grown on Si is under biaxial tension. The strain lifts the sixfold degeneracy in the conduction band and lowers the two perpendicular valleys (labeled Δ_2 in Fig. 1) with respect to the four in-plane valleys (Δ_4). Electrons are expected to preferentially occupy the lower-energy Δ_2 valleys, reducing the effective in-plane transport mass. The energy splitting also suppresses intervalley phonon-carrier scattering, increasing the electron low-field mobility.

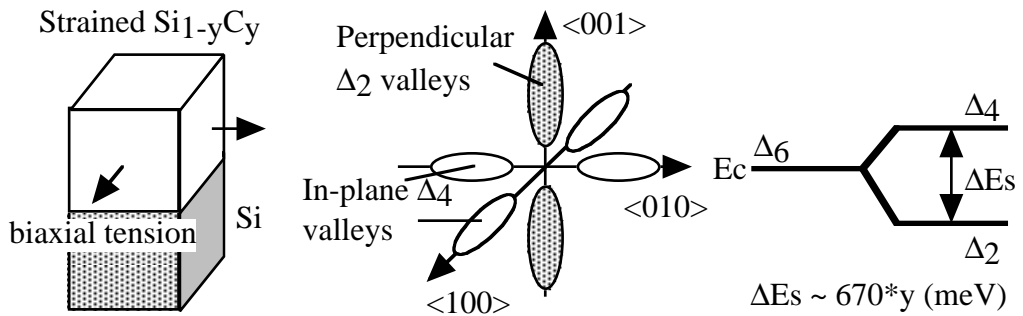


Fig. 1: Schematic illustrations of strained $\text{Si}_{1-y}\text{C}_y$.

To study in-plane electron transport in the strained undoped $\text{Si}_{1-y}\text{C}_y$ layer grown on the Si (001) substrate, we used an ensemble Monte Carlo simulation. Conduction band structure and physical parameters of the $\text{Si}_{1-y}\text{C}_y$ alloy were assumed to be the same as those of Si since the carbon fraction y in the present study was as small as 1 at. %. Acoustic phonon, intervalley f - and g -type phonon scattering, were included in the present model and alloy scattering was neglected in the calculation. The velocity-field and velocity-time characteristics are shown in Figs. 2 (a) and (b), respectively. The temperature and the carbon fraction was assumed to be 300 K and 1 at. %, respectively. The low-field electron mobility of Si is 1200 cm²/Vs while that of strained $\text{Si}_{0.99}\text{C}_{0.01}$ is 1600 cm²/Vs, as shown in Fig. 2 (a). Furthermore, the velocity-overshoot effect is enhanced in the strained $\text{Si}_{1-y}\text{C}_y$.

These superior features of strained $\text{Si}_{1-y}\text{C}_y$ cause the improvement of device performance not only submicron but also deep submicron MOS device. Next, we will describe the epitaxial growth of $\text{Si}_{1-y}\text{C}_y$.

3 Experimental

Epitaxial $\text{Si}_{1-y}\text{C}_y$ films were grown by CVD methods using a gas mixture of SiH_4 and H_2 . The C addition was carried out using C_2H_2 , CH_4 or $\text{SiH}_2(\text{CH}_3)_2$. In this report, we mainly describe the epitaxial growth with C_2H_2 gas. For the mercury sensitized photo-CVD method, the light source was a low-temperature Hg lamp radiating 254 nm (40 mW/cm²) and 185 nm (less than 10 mW/cm²) resonance lines. The SiH_4 flow rate was maintained at 10 sccm. H_2 and C_2H_2 flow rates were 3–40 sccm and 0–0.1 sccm,

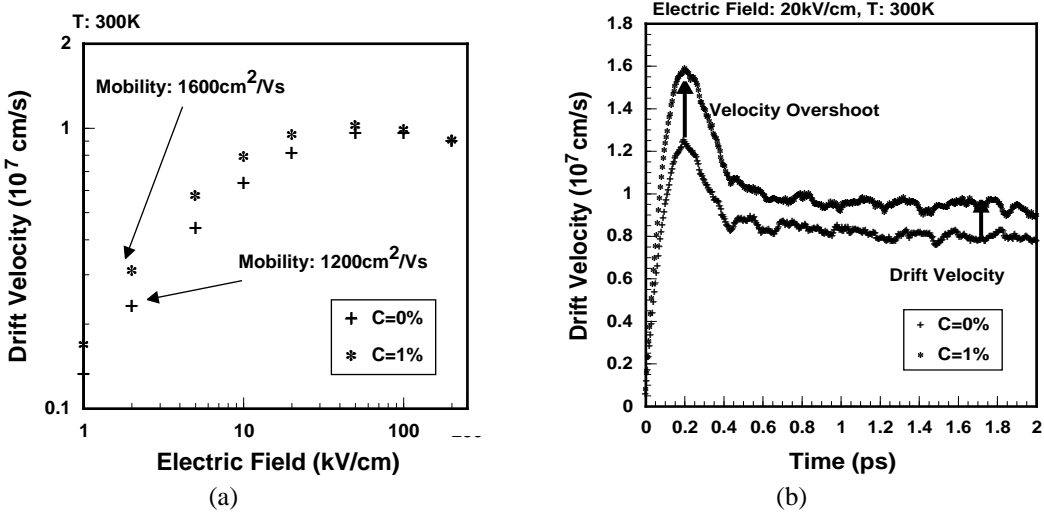


Fig. 2: Electron transport properties of strained $\text{Si}_{1-y}\text{C}_y$.

respectively. The substrate temperature was 225°C. For the plasma-CVD method, the electrode distance of 40 mm and RF plasma power of 127 mW/cm² were used. The SiH_4 flow rate was maintained at 2 sccm. H_2 and C_2H_2 flow rates were 17–160 sccm and 0–0.1 sccm, respectively. The substrate temperature was 210°C. For both methods, the films were grown on floating zone (FZ) n-type Si(100) substrates which were cleaned in organic solvents, etched by 20 % hydrofluoric (HF) acid and rinsed in deionized (DI) water for *ex situ* preparation. No *in situ* treatments were carried out. The growth rate was about 0.1 nm/s and the film thickness was about 200 nm.

The epitaxial growth was confirmed by reflection high-energy electron diffraction (RHEED). The optical and structural properties were measured by Fourier transform infrared absorption spectroscopy (FT-IR), Raman scattering spectroscopy and high-resolution X-ray diffractometry (HRXRD) using copper K_α X-rays. The distribution of the elements within the films was characterized by secondary ion mass spectroscopy (SIMS).

4 Results and Discussion

Figure 3 shows the dependence of the film structure on both the flow rate ratio of C_2H_2 to SiH_4 and the flow rate ratio of H_2 to SiH_4 . The solid lines in the figure indicate the epitaxial-amorphous boundary of the film structure. It was shown in our previous work that atomic hydrogen was required for low-temperature Si epitaxy [7]. Thus, the result shows that more H_2 dilution is required for epitaxy by the two CVD methods with increasing C addition and that the amount of H atoms in the gas phase or on the growth surface is reduced by reactions with C-based radicals generated from C_2H_2 .

The IR spectra of the as-grown and annealed samples grown by plasma-CVD with a $\text{C}_2\text{H}_2/\text{SiH}_4$ ratio of 0.005 are shown in Fig. 4. It is well known that a vibration mode at 607 cm⁻¹, indicating C atoms at the Si substitutional sites, is observed in the $\text{Si}_{1-y}\text{C}_y$ alloy [12]. An IR peak at 1950 cm⁻¹ originating from the Si-H_x configuration is observed in the as-grown sample. This IR peak disappears in the film annealed at 500°C, indicating the desorption of H atoms from the film. This IR observation corresponds well to the

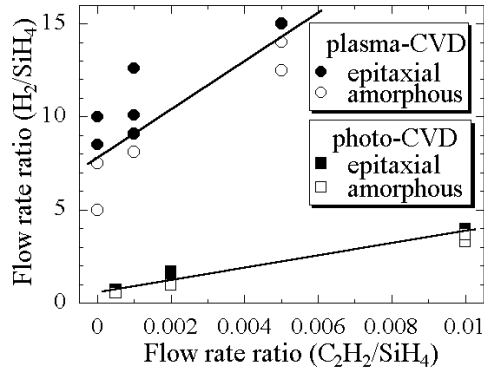


Fig. 3: Dependence of film structure both on the $\text{C}_2\text{H}_2/\text{SiH}_4$ and on H_2/SiH_4 .

XRD results, as indicated below. The C vibration mode at 607 cm^{-1} is observed in the annealed sample but not in the as-grown sample. The Raman spectra also show the same vibration mode in the samples annealed at 600°C , indicating that part of the incorporated C atoms are located at the Si substitutional sites.

The XRD (004) spectra are shown in Fig. 5. It is expected that the C incorporation into the Si layer will decrease the lattice constant. However, the XRD peak of the epitaxial $\text{Si}_{1-y}\text{C}_y$ films is shifted to a lower degree compared to the peak of the substrate. In our previous work, we found that the lattice of low-temperature Si epitaxial film is expanded by incorporated H atoms in the center of the Si-Si bond [13]. This is due to increasing H incorporation with increasing the addition of C_2H_2 . In order to desorb the H in the films, we carried out thermal annealing in N_2 atmosphere. The XRD peak positions of the epitaxial $\text{Si}_{1-y}\text{C}_y$ layer and the substrate are of the same order after annealing at 500°C . These results indicate the desorption of H atoms in the Si-Si bond by annealing. The XRD pattern of the layer annealed at 700°C reveals that the lattice constant is smaller than that of Si.

The lattice constant of the annealed $\text{Si}_{1-y}\text{C}_y$ layer decreases with increasing $\text{C}_2\text{H}_2/\text{SiH}_4$ ratio, as shown in Fig. 6. The formation of $\text{Si}_{1-y}\text{C}_y$ alloy is confirmed from these results. We have obtained similar FT-IR, Raman spectra and XRD measurement results for the samples grown by photo-CVD. The sub-

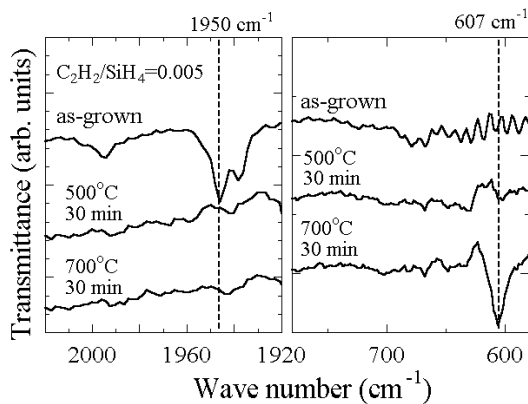


Fig. 4: IR spectra of the as-grown and the annealed samples grown by plasma-CVD.

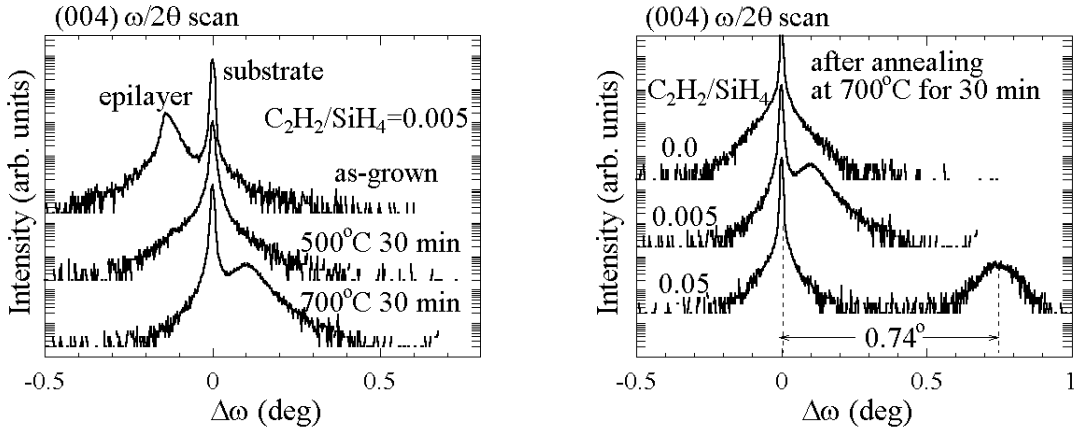


Fig. 5: XRD(004) spectra of $\text{Si}_{1-y}\text{C}_y$ as a function of annealing temperature.

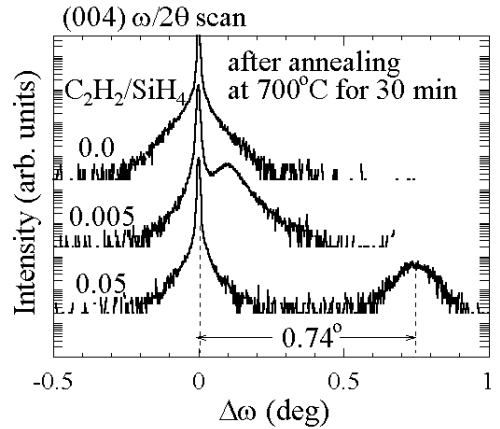


Fig. 6: XRD(004) spectra of annealed $\text{Si}_{1-y}\text{C}_y$ as a function of C fraction.

stitutional C compositions were calculated considering the strain in the films using Vegard's law, which is based on the lattice constants of Si and 3C-SiC. The maximum substitutional C compositions of about 2.3 at. % and 2.7 at. % were obtained by the mercury sensitized photo-CVD and plasma-CVD, respectively. Furthermore, we obtained C fraction of 3.5 at. % with $\text{SiH}_2(\text{CH}_3)_2$ as a C source gas by plasma-CVD. We ascertained that the crystallinity of these annealed samples was also epitaxial by RHEED observations, which revealed streak patterns. The ratio of the substitutional C composition compared with the total C composition estimated by SIMS was about 50–70 %.

5 Summary

$\text{Si}_{1-y}\text{C}_y$ films were grown on Si(001) by mercury sensitized photo-CVD and plasma-CVD at substrate temperatures of around 200°C. We found that the hydrogen dilution ratio required for epitaxial growth increased with increasing the $\text{C}_2\text{H}_2/\text{SiH}_4$ ratio. FT-IR and Raman spectra of the samples annealed at 600–700°C showed the C local vibration mode at 607 cm^{-1} , indicating that part of the C atoms were located at the Si substitutional site. XRD patterns revealed that the lattice constant of the layer annealed at 700°C was smaller than that of Si. The formation of $\text{Si}_{1-y}\text{C}_y$ alloy was confirmed from these results. Control of the C composition was achieved by varying the $\text{C}_2\text{H}_2/\text{SiH}_4$ ratio. The maximum substitutional C compositions of 3.5 at. % was successfully obtained by plasma-CVD with $\text{SiH}_2(\text{CH}_3)_2$ gas.

References

- [1] K. Rim, J. L. Hoyt and J. F. Gibbons: IEEE Trans. Electron Dev. **47** (2000) 1406.
- [2] J. P. Dismukes, J. Ekstrom, E. F. Steigmeier, I. Kudman and D. S. Beers: J. App. Phys. **35** (1964) 2899.
- [3] H. J. Osten, J. Griesche and S. Scalese: Appl. Phys. Lett. **74** (1999) 836.

- [4] A. C. Mocuta and D. W. Greve: *J. Appl. Phys.* **85** (1999) 1240.
- [5] K. B. Joelsson, W. Ni, G. Pozina, L. Hultman and G. V. Hansson: *Vacuum* **49** (1998) 185.
- [6] J. L. Hoyt, T. O. Mitchell, K. Rim, D. V. Singh and J. F. Gibbons: *Thin Solid Films* **321** (1998) 41.
- [7] T. Oshima, A. Yamada and M. Konagai: *Jpn. J. Appl. Phys.* **36** (1997) 6481.
- [8] Y. Jia, T. Oshima, A. Yamada, M. Konagai and K. Takahashi: *Jpn. J. Appl. Phys.* **32** (1993) 1884.
- [9] T. Watahiki, A. Yamada and M. Konagai: *J. Cryst. Growth* **209** (2000) 335.
- [10] A. Yamada, Y. Jia, M. Konagai and K. Takahashi: *Jpn. J. Appl. Phys.* **28** (1989) L2284.
- [11] T. Oshima, K. Abe, A. Yamada and M. Konagai: *Jpn. J. Appl. Phys.* **34** (1995) L1425.
- [12] M. Meléndez-Lira, J. D. Lorentzen, J. Menéndez, W. Windl, N. G. Cave, R. Liu, J. W. Christiansen, N. D. Theodore and J. J. Candelaria: *Phys. Rev. B* **56** (1997) 3648.
- [13] K. Abe, T. Watahiki, A. Yamada and M. Konagai: *Jpn. J. Appl. Phys.* **37** (1998) 1202.